

## LA-UR-21-24414

Approved for public release; distribution is unlimited.

Title: The Snell's Law Shell Ionospheric Transfer Function

Author(s): Light, Max Eugene

Intended for: Report

Issued: 2021-05-06

---

**Disclaimer:**

Los Alamos National Laboratory, an affirmative action/equal opportunity employer, is operated by Triad National Security, LLC for the National Nuclear Security Administration of U.S. Department of Energy under contract 89233218CNA000001. By approving this article, the publisher recognizes that the U.S. Government retains nonexclusive, royalty-free license to publish or reproduce the published form of this contribution, or to allow others to do so, for U.S. Government purposes. Los Alamos National Laboratory requests that the publisher identify this article as work performed under the auspices of the U.S. Department of Energy. Los Alamos National Laboratory strongly supports academic freedom and a researcher's right to publish; as an institution, however, the Laboratory does not endorse the viewpoint of a publication or guarantee its technical correctness.

# The Snell's Law Shell Ionospheric Transfer Function

Max Light

April 7, 2021

## 1 Introduction

Ionospheric transfer function (ITF) algorithms determine the effects of the ionosphere on an electromagnetic (EM) radio-frequency (RF) signal as it propagates through. In this report, the Snell's law shell (slab) model is outlined.

This algorithm is expressed in the frequency domain. In this way, it is applied as linear time invariant (LTI) filter function [3].

Signals in this report are assumed to have only a single component (i.e.  $x$ ,  $y$  or  $z$  in a rectangular coordinate system). Multi-component signals can be treated simply by applying the specific ITF to each component separately.

## 2 Snell's law shell algorithm

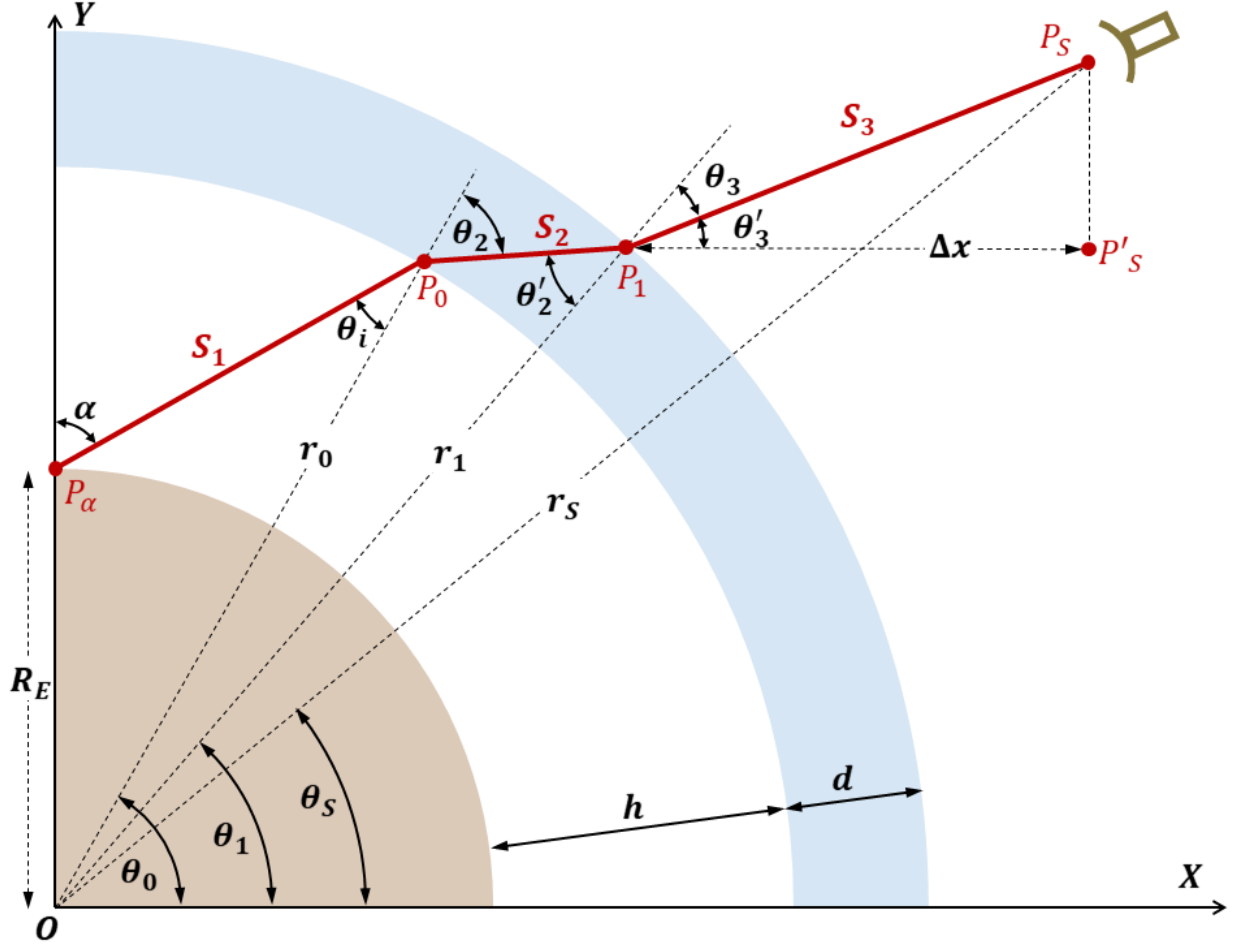


**Figure 1:** Geometry for the Snell's law shell model. The configuration for a ray that hits the satellite is shown.

Consider an EM signal originating at a point source and traversing the ionosphere to a detector, as shown in figure 1. The ionosphere is represented by the blue region and is assumed to be a homogeneous spherical shell of some arbitrary thickness  $d$ , starting at a radius  $h$  relative to the earth's surface at radius  $R_E$ , with a constant plasma electron density  $n_0$  in a two dimensional geometry. Electron collisions and ion motions will be ignored in this treatment because ions are considered to be too massive to contribute to phenomena on the time scale of the RF EM wave, and wave damping due to electron collisions is assumed insignificant. In rectilinear coordinates, the signal path is

$$P_\alpha(0, R_E) \longrightarrow P_0(x_0, y_0) \longrightarrow P_1(x_1, y_1) \longrightarrow P_S(x_S, y_S) \quad (1)$$

or in cylindrical coordinates

$$P_\alpha(R_E, 0) \longrightarrow P_0(r_0, \theta_0) \longrightarrow P_1(r_1, \theta_1) \longrightarrow P_S(r_S, \theta_S) \quad (2)$$

It travels a total distance  $S = S_1 + S_2 + S_3$ . Thus, the signal amplitude is decreased by a factor  $1/S$ . This is not strictly correct, as it does not account for the increase in the flux tube encompassed by the ray as it propagates outward in the  $r$  coordinate. However, for the purposes of this report, this assumption is strong enough to be considered valid for the change in signal amplitude. The Earth's magnetic field is assumed to be constant through the shell, with a magnitude of  $B_0$ . The angle  $\beta$  between the LOS and  $B_0$  is therefore also a constant.

To summarize, the assumptions used above are

- **PLASMA** The ionosphere is a shell of constant density plasma with massive ions and collisionless electrons.
- **MAGNETIC FIELD** The Earth's magnetic field is a constant.
- **$B_0$  ORIENTATION** The angle between the Earth's magnetic field and the line of sight does not change.

The index of refraction  $\mathbf{n}_p(\omega)$  in the plasma for either fast ( $\mathbf{m} = -1$ ) or slow ( $\mathbf{m} = +1$ ) root is given by the Appleton Hartree dispersion relation [1]

$$\mathbf{n}_p(\omega) = \sqrt{1 - \frac{X(\omega)}{1 - \frac{1}{2} \frac{Y^2(\omega) \sin^2 \beta}{1 - X(\omega)} + \mathbf{m} \left[ \frac{1}{4} \frac{Y^4 \sin^4 \beta}{(1 - X(\omega))^2} + Y^2(\omega) \cos^2 \beta \right]^{1/2}}} \quad (3)$$

In the above equation, the plasma and cyclotron frequencies are

$$\omega_p^2 = \frac{n_0 q^2}{\epsilon_0 m_e} \quad \text{and} \quad \omega_c = \frac{q B_0}{m_e} \quad (4)$$

where  $\epsilon_0$ ,  $m_e$ , and  $q$  are the permittivity and free space, electron mass, and electron charge in MKS units respectively.

In addition, the two dimensional geometry is constructed so that the source is located at point  $P$  at  $(0, R_E)$  where  $R_E$  is the Earth's radius. This configuration is easily realized with the appropriate coordinate rotation. The ionosphere begins at an altitude  $h = r_0 - R_E$  with a width  $d$ .

The signal path (Poynting vector) is refracted according to Snell's law at the bottom and top sides of the ionosphere. The Poynting vector direction of propagation can be treated like a ray path under the geometric optics assumption [4, 1], which is valid for this construction and frequency range.

Consider an EM signal ray launched at an inclination angle of  $\alpha$  at point  $(0, R_E)$  as shown in figure 1, which intersects the satellite detector. A straightforward application of geometry along the radial coordinate to the satellite, and Snell's law at points  $P_0$  (bottom) and  $P_1$  (top), will lead to the geometric expression of the ray's path.

To begin,  $S_1$  is calculated in terms of the underside pierce point

$$S_1 = \frac{x_0}{\sin \alpha} \quad (5)$$

The radius from the origin to that point is given by the law of cosines

$$r_0^2 = R_E^2 + S_1^2 - 2R_E S_1 \cos(\pi - \alpha) \quad (6)$$

$$= R_E^2 + S_1^2 + 2R_E S_1 \cos(\alpha) \quad (7)$$

Using equation 5, and  $r_0 = R_E + h$ , in equation 7 gives a quadratic equation for  $x_0$  in terms of  $\alpha$

$$x_0 = -\frac{R_E}{2} \sin 2\alpha \pm \frac{1}{2} \sin 2\alpha \left[ R_E^2 + \frac{h^2 + 2R_E h}{\cos^2 \alpha} \right]^{1/2} \quad (8)$$

Discard the nonphysical (negative) root to get

$$x_0 = -\frac{R_E}{2} \sin 2\alpha + \frac{1}{2} \sin 2\alpha \left[ R_E^2 + \frac{h^2 + 2R_E h}{\cos^2 \alpha} \right]^{1/2} \quad (9)$$

Next, from the law of sines

$$\frac{R_E}{\sin \theta_i} = \frac{r_0}{\sin(\pi - \alpha)} \quad (10)$$

such that the incident underside pierce point angle is

$$\theta_i = \sin^{-1} \left( \frac{R_E}{r_0} \sin \alpha \right) \quad (11)$$

Now, according to Snell's law at the underside pierce point,  $P_0$ ,

$$1 \cdot \sin \theta_i = \mathbf{n}_p \sin \theta_2 \quad (12)$$

where the frequency dependence of  $\mathbf{n}_p$  is assumed, and  $n_0 = 1$ . Thus

$$\theta_2 = \sin^{-1} \left( \frac{1}{\mathbf{n}_p} \sin \theta_i \right) = \sin^{-1} \left( \frac{R_E}{r_0 \mathbf{n}_p} \sin \alpha \right) \quad (13)$$

Again, from the law of sines,

$$\frac{r_1}{\sin(\pi - \theta_2)} = \frac{r_0}{\sin \theta_2'} \quad (14)$$

so the equation for the angle  $\theta_2'$  is

$$\theta_2' = \sin^{-1} \left( \frac{r_0}{r_1} \sin \theta_2 \right) \quad (15)$$

Next, let  $\Delta\theta = \theta_0 - \theta_1$  and consider the triangle given by  $OP_0P_1$ . The sum of the interior angles is  $\pi$ , so that

$$\begin{aligned} \theta_2' + \pi - \theta_2 + \Delta\theta &= \pi \\ \Rightarrow \theta_2' + \pi - \theta_2 + \theta_0 - \theta_1 &= \pi \\ \Rightarrow \theta_1 &= \theta_0 + \theta_2' - \theta_2 \end{aligned} \quad (16)$$

and the final form of  $\theta_1$  is found by using eqns. 13 and 15 in the above result

$$\theta_1 = \cos^{-1} \left( \frac{x_0}{r_0} \right) + \sin^{-1} \left( \frac{R_E}{\mathbf{n}_p r_1} \sin \alpha \right) - \sin^{-1} \left( \frac{R_E}{\mathbf{n}_p r_0} \sin \alpha \right) \quad (17)$$

Once again, the law of cosines gives

$$S_2 = \left( r_0^2 + r_1^2 - 2r_0 r_1 \cos \Delta\theta \right)^{1/2} \quad (18)$$

$$= \left( r_0^2 + r_1^2 - 2r_0 r_1 \cos(\theta_0 - \theta_1) \right)^{1/2} \quad (19)$$

At point  $P_1$ , Snell's law is

$$\mathbf{n}_p \sin \theta'_2 = 1 \cdot \sin \theta_3 \quad (20)$$

and using equations 11, 13, and 15 in the above equation results in the expression for the angle  $\theta_3$

$$\theta_3 = \sin^{-1} \left( \frac{R_E}{r_1} \sin \alpha \right) \quad (21)$$

Now, from triangle  $P_1 P'_s P_s$  and the law of sines

$$\frac{S_3}{\sin \pi/2} = \frac{y_S - y_1}{\theta'_3} \quad (22)$$

note that  $\theta'_3 = \theta_1 - \theta_3$  and  $y_1 = r_1 \sin \theta_1$ . Using these in the above equation gives the expression for  $S_3$

$$S_3 = \frac{y_S - r_1 \sin \theta_1}{\sin (\theta_1 - \theta_3)} \quad (23)$$

Thus, given the satellite detector coordinates  $(r_S, \theta_S)$ , the ray that intersects the detector follows segments  $S_1, S_2$ , and  $S_3$ . These segments are located using the angles and lengths found in equations 5 to 23. Note that first: all the parameters are functions of the launch angle  $\alpha$ , and second: the detector location can be found in two ways. Consider the  $x$  coordinate. It is found from the detector coordinates

$$x_S = r_s \cos \theta_S \quad (24)$$

but can also be found using the derived expressions for the ray path

$$\begin{aligned} x_S &= x_1 + \Delta x \\ &= r_1 \cos \theta_1 + S_3 \cos \theta'_3 \\ &= r_1 \cos \theta_1 + \frac{y_S - r_1 \sin \theta_1}{\tan (\theta_1 - \theta_3)} \end{aligned} \quad (25)$$

Equating the right hand side expressions in equations 24 and 25 results in a conditional equation that depends on  $\alpha$

$$r_s \cos \theta_S \stackrel{?}{=} r_1 \cos \theta_1(\alpha) + \frac{y_S - r_1(\alpha) \sin \theta_1(\alpha)}{\tan (\theta_1(\alpha) - \theta_3(\alpha))} \quad (26)$$

and will be called the constraint equation from here on. It is solved iteratively, at every frequency in the signal bandwidth, to find the launch angle  $\alpha$  for the ray to intersect the satellite. Note that this angle may not exist depending on the detector position and parameters of the ionosphere shell.

Each frequency component of the signal that intersects the detector will then have its amplitude decreased by a factor

$$\frac{1}{S_1 + S_2 + S_3}$$

The phase of those components is calculated using the phase velocity of the signal on each segment of the ray. This velocity is the speed of light for segments  $S_1$  and  $S_3$ , while it is given by the phase velocity of an EM wave in a magnetized plasma with the parameters specified by the ionosphere shell for segment  $S_2$ .

### 3 solving the constraint equation

There are many methods for iteratively solving the constraint equation, 26. There are some important points to consider as well. From figure 1 and Snell's law at a vacuum/plasma interface, it is clear that any ray path originating from the point  $(0, RE)$  will refract in the clockwise direction at the underside of the ionosphere shell. This means that for the ray to intersect the detector, the maximum in  $\alpha$  is defined as the angle between the  $y$  axis and the line of sight to the detector  $\alpha_{SAT}$ , and this would be for no refraction in the ionosphere, so it is an absolute upper limit (see figure 2).

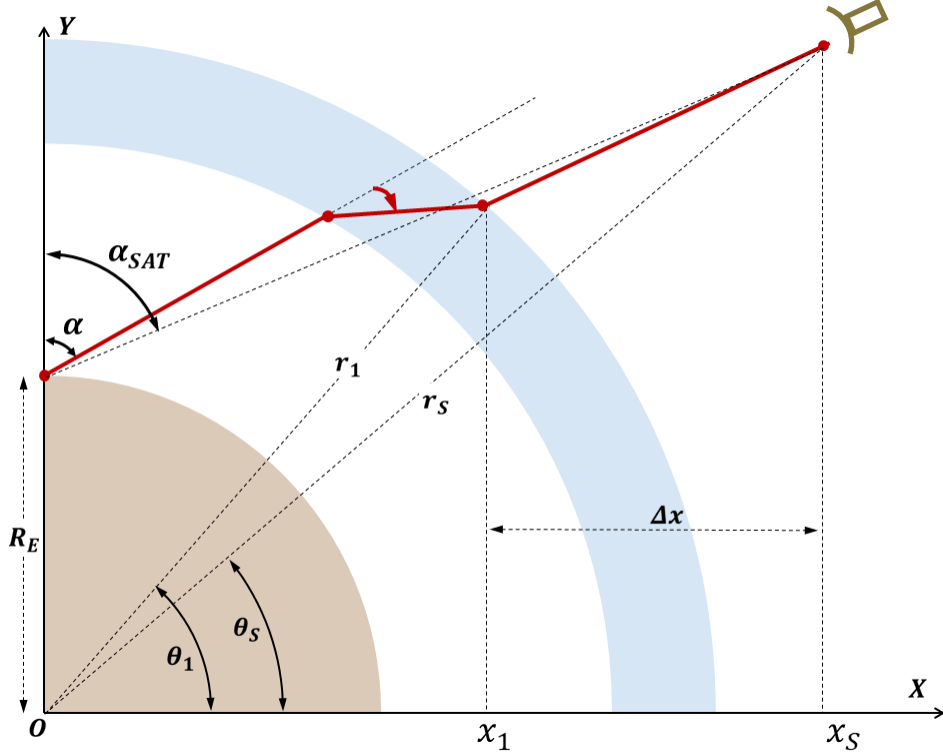


**Figure 2:** Geometry for the Snell's law shell model. Showing the relation between  $\alpha$  and  $\alpha_{SAT}$ .

The next item to consider is that once  $\theta_2$  in figure 1 becomes equal to or greater than  $\pi/2$ , the ray has suffered complete reflection at the vacuum/plasma interface at the underside of the ionosphere shell. Thus  $\theta_2(\alpha) < \pi/2$  for a ray to have a nonzero probability of reaching the detector. Equation 13 can be used in equation 11 to get

$$\theta_2(\alpha) = \sin^{-1} \left( \frac{R_E}{n_p R_0} \sin \alpha \right) \leq \frac{\pi}{2} \quad (27)$$

or, in terms of the angle  $\alpha$

$$\alpha \leq \sin^{-1} \left( \frac{n_p R_0}{R_E} \right) \quad (28)$$

Equations 27 and 28 define the upper limit on the angle  $\alpha$ , whichever is smaller. The  $\alpha$  root



that solves the constraint equation can be bracketed in the interval

$$\begin{aligned} & [0, \alpha_{SAT}] \quad , \quad \alpha_{SAT} < \sin^{-1} \left( \frac{\mathbf{n}_p R_0}{R_E} \right) \\ & \left[ 0, \sin^{-1} \left( \frac{\mathbf{n}_p R_0}{R_E} \right) \right] \quad , \quad \alpha_{SAT} \geq \sin^{-1} \left( \frac{\mathbf{n}_p R_0}{R_E} \right) \end{aligned}$$

With this knowledge, the bisection algorithm was chosen to solve the constraint equation, 26, numerically. Thus, at each frequency step in the signal bandwidth, the bisection method is used to find the existence of a root  $\alpha$ . If that root exists, then the ray at that frequency intersects the satellite detector. The tolerance in finding the root is set to be several orders of magnitude less than a degree.

## References

- [1] K. G. Budden.  
*The Propagation of Radio Waves*.  
Cambridge University Press, 1985.
- [2] Ronald Moses and Abram Jacobson.  
Ionospheric profiling through radio-frequency signals recorded by the FORTÉ satellite, with  
comparison to the international reference ionosphere.  
*Advances in Space Research*, 34:2096–2103, 12 2004.
- [3] F. G. Stremler.  
*Introduction to Communication Systems*.  
Addison-Wesley, second edition, 1982.
- [4] D. G. Swanson.  
*Plasma Waves*.  
Institute of Physics, second edition, 2003.